Exp Fluids (2012) 52:85–94
DOI 10.1007/s00348-011-1202-3

RESEARCH ARTICLE

Experimental study of near-wall turbulent characteristics in an open-channel with gravel bed using an acoustic Doppler velocimeter

X. Y. Wang · Q. Y. Yang · W. Z. Lu · X. K. Wang

Received: 30 November 2010 / Revised: 9 September 2011 / Accepted: 12 September 2011 / Published online: 29 September 2011
© Springer-Verlag 2011

Abstract This experimental study investigated the mean velocity profiles, skin friction and turbulent characteristics of a gravel bed over a wide range of roughness using an acoustic Doppler velocimeter (ADV). The median diameter of bed material ranged from 2 to 40 mm, and the normalized roughness heights ranged from 47 to 4,881 mm. The flow regime was fully developed turbulence with a Reynolds number in the range of 4.2×10^4–9.86×10^4. All velocity curves exhibited logarithmic distributions, and the log-law region was influenced greatly by both the roughness and the Reynolds number. Moreover, the roughness of the gravel bed exerted a strong effect on Reynolds stress, and the turbulence tended towards isotropic with increasing roughness. Using statistical analyses, the third-order turbulence moments, sweep, and ejection motions were also examined. The results of this experimental analysis present a contrast to the classical wall similarity hypothesis.

X. Y. Wang
State Key Laboratory of Estuarine and Coastal Research, East China Normal University, Shanghai 200062, People's Republic of China

X. Y. Wang · Q. Y. Yang · W. Z. Lu (✉)
Department of Civil and Architectural Engineering, City University of Hong Kong, Kowloon, Hong Kong, SAR, People's Republic of China
e-mail: bcwzlu@cityu.edu.hk

X. K. Wang
State Key Laboratory of Hydraulics and Mountain River Engineering, Sichuan University, Chengdu 610065, People's Republic of China

1 Introduction

The flow characteristics of turbulent flow over gravel beds merit much attention and research due to their significant applications in industry and engineering (Blocken et al. 2007; Hong et al. 2011; Lu and Leung 2003; Nikora and Smart 1997; Tritico and Hotchkiss 2005). Turbulence in gravel bed flow is influenced greatly by surface roughness, and the flow structure is much more complicated than that in smooth walls. Though many issues have been well studied and documented (Perry et al. 1969; Nezu and Nakagawa 1993; Ferro and Baiamonte 1994; Tachie et al. 2000; Volino et al. 2009), the flow structure under large roughness conditions still needs to be addressed in order to further understand near-bed processes.

As indicated in a review by Jimenez (2004), the biggest effects of roughness are the change in mean velocity profile near the wall and the friction coefficient, which was well studied by Ferro (1999) and (2003a). In smooth open channels, it is well known that the near-wall region can be divided into a viscous subrange, buffer layer and log layer (Nakagawa et al. 1975; Nezu and Nakagawa 1993). Flow patterns in the different layers have distinct characteristics. According to Prandtl's mixing length theory, the mean velocity profile can be derived and expressed as:

$$U^+ = \frac{1}{\kappa}\ln(y^+) + B \qquad (1)$$

where $U^+ = U/U_\tau$, $y^+ = yU_\tau/\nu$, $U_\tau = \sqrt{\tau_w/\rho}$, U_τ is the shear velocity or friction velocity, τ_w is the wall shear stress, and ρ is the fluid density. Equation 1 is known as the "log-law" and fits well with experimental data under smooth-wall conditions. For a rough wall, the roughness elements alter the flow structure in near-wall region substantially. Consequently, a roughness function ΔU^+ is defined and added to describe the velocity profile (Shocking et al. 2006). The roughness function is normally a function of roughness length k_s (representative roughness height). Therefore the log-law in a rough wall becomes:

$$U^+ = \frac{1}{\kappa}\ln(y^+) + B - \Delta U^+ \quad (2)$$

It was further shown that Eq. 1 is applicable to a two-dimensional smooth wall with a zero-pressure-gradient, and Eq. 2 to mesh or to a rod-roughened wall (Antonia 2001; Ferro 2003b; Flack et al. 2005). It should be noted that the von Karman constant κ and integral constant B are not invariable, but rather are Reynolds number dependent (Wosnik et al. 2000; Nagib et al. 2006). Moreover, the roughness length k_s, with various values (van Rijn 1982), is difficult to determine, especially in non-uniform beds. As one of the most important parameters, the friction velocity U_τ must be estimated carefully (Castillo et al. 2004; Brzek et al. 2007). The shear velocity is also used to estimate the flow resistance relating to the skin friction factor C_f (Cal et al. 2009). Besides the uncertainties of these latter parameters, the hold region of the log-law is a range that depends on the roughness element, the relative depth (ratio of flow depth to roughness height), and the Reynolds number (Ferro and Baiamonte 1994; Zanoun et al. 2003). In certain large-roughness gravel beds, velocity profiles may even deviate from log-law (Ferro 2003b).

In open channel flow, near-bed turbulence characteristics are difficult to measure by virtue of the irregular surface protrusions. The macro-turbulent events induced by roughness, such as sweep and ejection motions, prevail close to the rough wall. Thanks to the flow visualization technique, the vortices caused by the gravel obstacles are observed to be responsible for the interaction mechanism between the inner zone and the outer zone (Kirkbride 1993; Kirkbride and McLelland 1994; Tachie et al. 2000; Sheng et al. 2008; Hong et al. 2011). The large-scale eddies in gravel beds can affect both turbulence and sediment transport (Shvidchenko and Pender 2001). Expressions of turbulence intensity and Reynolds stresses have been derived theoretically (Bandypadhyay and Watson 1988; Bakken et al. 2005; Carollo et al. 2005; Dey and Lambert 2005); however, in non-uniform open-channel flow experiments, Song et al. (2001) confirmed that the Reynolds stresses were smaller than those calculated from theoretical equations. Besides the distribution discrepancies, the limit of roughness effect on turbulence is also controversial. According to the wall similarity hypothesis (Townsend 1976; Raupach 1981; Lopez and Garcia 1999), turbulence, with several roughness heights away from the wall bottom, is independent of surface conditions at high Reynolds numbers, which corresponds to the concept that the effective limit of roughness on turbulence structure is restricted to a roughness sublayer (Nezu and Nakagawa 1993). Many experimental results support this view, including field measurements (Nikora and Smart 1997; Smart 1999; Stone et al. 2003; Tritico and Hotchkiss 2005; Volino et al. 2007) and flume experiments in the laboratory (Franca 2005; Schultz and Flack 2005, 2007; Flack et al. 2007; Wu and Christensen 2007). Besides, Flack et al. (2005) suggested that this limit should be less than $3k_s$, and that higher-order moments be confined to $y < 5k_s$. The third-order moments of Bakken et al. (2005) were also confirmed to obey this hypothesis. However, certain controversial points remain to be addressed on this issue. Krogstad et al. (1992) and Krogstad and Antonia (1999) stated, from experiments, that roughness can extend its effect into the outer region. Wang (1991) and Wang and Dong (1996) indicated that the turbulent intensity depends greatly on the relative roughness. Clarification of this issue needs more systematic experiments covering a large range of roughness.

The Doppler shift principle provides the capability to measure undisturbed velocity instantaneously. The acoustic Doppler velocimeter (ADV), which can simultaneously obtain three-dimensional velocities at high frequency, has been applied successfully in gravel beds (Nezu and Rodi 1986; Lane et al. 1998; Carollo et al. 2005; Leonardi et al. 2005; Bigillon et al. 2006). Given appropriate post-processing (Nikora et al. 1998; McLelland and Nicholas 2000), the ADV technique can be used for turbulence measurements. In addition, statistical analysis can also be used to examine turbulent fluctuations as well as quantitative evidence of coherent structure.

Although some studies on the flow characteristics in rough beds, including mesh, rod and artificial roughness (Lyn 1993), have been reported, research into extremely large-scale, three-dimensional rough conditions is limited. The aim of this study was to investigate the mean flow and turbulence characteristics over a gravel bed. The rough surfaces here consist of uniform sediment particles. The hydraulic regime is fully developed turbulent, open-channel flow. The experimental results can be used to better understand the flow structure in rough beds, and could help to efficiently predict turbulent flow in numerical simulations.

2 Experimental setup and methodology

The experiments were conducted in a circulation system located in the State Key Laboratory of Hydraulics and

Mountain River in Sichuan University, China. The experiments were carried out in a flat flume 0.60 m wide, 0.60 m deep and 13.5 m long. The test section located in the middle of the flume, where the flow was in fully developed turbulent regime, was 4.0 m long, and 0.6 m wide. The water was driven by a pump capable of providing a flow discharge up to 100 L s^{-1}. Water was first pumped from the tank into a static pool and then passed through the baffle to suppress the fluctuation before it entered the flume. At the outlet of the flume, a tailgate was installed to maintain the flow depth.

The gravel beds consisted of sorted uniform sediments in each experiment ranging from 2 to 40 mm. To prevent local scour, sections of 0.5 m near the inlet and outlet in the beds were made immobile. Prior to each experiment, the water level was carefully leveled up and the bed was then flowed for several hours with no sediment motion. To maintain identical bed configuration, variable runs were performed by changing the flow discharge and the flow depth. Figure 1 shows the experimental flume and a front view of the monitoring locations. The x, y and z indicate the longitudinal, lateral and vertical directions, respectively. Table 1 lists the relevant parameters of roughness length k_s, which is equal to the d_{50} (the diameter of bed particles at which 50% are smaller), the shear velocity U_τ, dimensionless $k_s^+ = k_s U_\tau / \nu$, the bulk free-stream velocity U_o, the Reynolds number $Re = RU_o/\nu$ (R is the hydraulic radius and ν is the kinematic viscosity), the Froude number $Fr = U_o/(gh)^{1/2}$ (g is the acceleration due to gravity), the flow depth h and the $Re_\theta = \theta U_0/\nu$ (θ is the momentum boundary layer thickness) of all runs.

The instantaneous velocities were measured by a three-dimensional, down-looking ADV mounted on a transverse boom so that it can be moved between the measurement points precisely. Velocity was monitored vertically from bed to the limited depth of equipment. The adopted SONTEK ADV measured the velocity 5 cm below the acoustic sensor. The probe volume was 0.09 cm^3, and the spatial resolution near the rough wall was 0.1 mm. With a frequency of 50 Hz, the time recorded was 20 s at each measurement point. The monitored signal was first transferred to the computer and then analyzed by WinADV software. As suggested (Voulgaris and Trowbridge 1998; Carollo et al. 2005), the data can be retained only when the signal-to-noise ratio (SNR) is greater than 15 dB and the correlation (COR) is greater than 70. Figure 2 depicts the typical power spectrum and probability density function (PDF)distribution of velocity. The overall uncertainty in the mean velocity is ±1% comparison with the laser Doppler velocimetry (LDV). The recorded length at 50 Hz sampling frequency is less than that suggested by Buffin-Belanger and Roy (2005). However, according to analysis of instantaneous-velocity standard errors, the calculated results were found to converge when the number of sample points was greater than 900. Statistical analysis was conducted to calculate the overall uncertainties, and the precision for turbulence characteristics is 95%. The uncertainty in C_f was ±7% according to statistical analysis.

Friction velocity is a key parameter used to normalize velocity variables, though currently it is difficult to estimate. In gravel beds, friction velocity is affected greatly by the morphological features of the bed. In this study, two different methods were used to estimate friction velocity. One is the turbulent-kinetic-energy (TKE) method, $\tau_0 = 0.5 C_1 \rho \left(\overline{u'^2} + \overline{v'^2} + \overline{w'^2} \right)$, where the coefficient C_1 is a constant and assumed to be 0.19, which is consistent with the value of Kim et al. (2000). In order to obtain this variable precisely, a detailed knowledge of near-wall turbulence characteristics is required. The other method is regression of velocity profiles in the near-wall region. This method has been proven to be applicable even in shallow rivers (Biron et al. 1998). Figure 3 provides the shear velocity estimation from these two methods, and the values calculated from the equilibrium equation are depicted on each axis. It can be seen that the results agree well with each other although small deviations exist at high values.

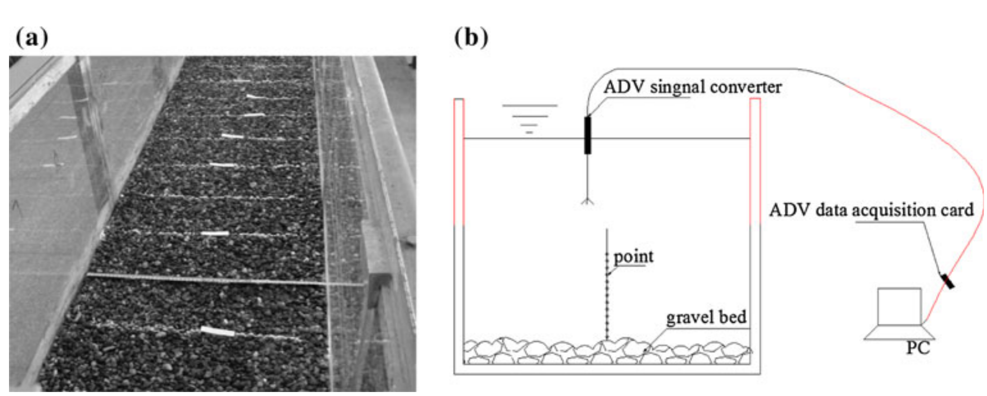

Fig. 1 Scheme of experiment. **a** Experimental flume, **b** monitoring setup. *ADV* Acoustic Doppler velocimeter

Table 1 Summary of experimental parameters

Run	k_s (mm)	k_s^+	*Re*	*Fr*	*H* (cm)	U_0 (cm/s)	U_τ (cm/s)	Re_θ	θ/k_s
1		–	51,530	0.15	50.2	34.0	1.49	2,056	–
2		–	71,782	0.35	29.3	60.0	2.41	3,127	–
3	2	47	51,130	0.18	42.0	36.2	2.40	2,131	364.70
4	5	164	60,305	0.24	37.0	45.1	3.33	2,969	163.15
5	5	250	71,554	0.42	24.8	65.3	5.10	3,813	144.68
6	10	401	44,300	0.33	19.6	46.3	4.10	3,368	90.14
7	10	470	70,783	0.33	30.7	57.8	5.60	3,608	77.34
8	10	568	68,148	0.46	21.9	66.7	6.10	5,595	103.92
9	10	876	96,039	0.73	19.4	101.0	8.90	6,860	84.15
10	20	762	53,201	0.24	31.8	42.7	4.50	3,967	57.55
11	20	1,521	97,540	0.51	27.9	83.6	7.70	5,192	38.48
12	20	1,976	97,560	0.74	19.4	102.6	9.00	8,106	48.95
13	20	1,154	74,362	0.38	28.1	63.5	5.30	7,181	70.05
14	40	1,432	42,012	0.21	28.8	35.4	3.80	5,852	51.21
15	40	2,518	75,043	0.37	29.5	62.5	6.10	8,118	40.23
16	40	4,884	98,573	0.84	17.5	110.5	13.60	6,885	19.30
17	40	4,361	98,308	0.72	20.1	101.2	15.00	6,463	19.78

3 Results and analysis

3.1 Mean velocity profiles

Experiments were carried out with varying flow discharge and water depth in each bed arrangement. Most of the beds employed in the experiments were in the fully rough range (i.e., $k_s^+ > 70$). The velocity profiles of all runs are depicted in Fig. 4. The roughness function in relation to roughness height is represented by solid lines in the figure. The mean velocity and vertical distance are normalized by shear velocity and inner scale ν/U_τ, respectively. The vertical distance is extended to the outer region so that the normalized vertical distance y^+ is up to 16,000. It can be seen that all profiles conform to the logarithmic distribution. Normally, in smooth wall, the log-law hold region is commonly considered as $30 < y^+ < 1{,}000$ (Blocken et al. 2007), while in gravel bed, it ranges from 150 to 10,000 as shown in Fig. 4. The log-law is commonly used to estimate the shear velocity using the regression method, but the region needs to be selected carefully. It is known that as the roughness increases, the friction velocity and y^+ also increase. This leads to an increase in the lower limit of the log-law hold region. In Fig. 4, the downward shifts from Run2 can be regarded as the value of roughness function. The values of roughness function depend on the roughness condition. It can also be observed that the roughness function, except for depending on the hydraulic conditions, is essentially proportional to the $\log_{10}(k_s^+)$. This conforms to the results of work by Krogstad and colleagues (Krogstad et al. 1992; Krogstad and Antonia 1999), which found that the roughness effect could be felt in the outer region even at high Reynolds number. This leads to the perception that turbulence is not only confined to a thin layer near the rough surface but is also affected by hydraulic conditions. Generally, the log-law is valid in the inner region, in which turbulence is fully developed. However, in gravel-bed rivers, the typical thickness of the viscous sublayer is 2.1×10^{-7} m (Kirkbride 1993). Furthermore, based on the condition of fully rough flow regions ($k_s^+ > 70$), the lower limit of the physical roughness height is $k_s = 3.8$ mm. This means that the viscous sublayer is almost absent in all gravel beds. Thus, the viscous sublayer disappears and a fluid layer termed the 'quasi-separated layer' is formed (Nezu and Nakagawa 1993). Detailed roughness effects should be investigated with more rough beds.

3.2 Skin friction and boundary layer relationships

Skin friction factor C_f is defined as the ratio of τ_w to $\rho U_0^2/2$, i.e., $C_f/2 = U_\tau^2/U_0^2$, where τ_w is the shear stress on bed and U_o is the bulk velocity. For rough surface, the skin friction is also related closely to the Reynolds number (Dean 1978; Schlichting 1979) and the relative depth (Ferro and Giordano 1991; Ferro 1999). Hence, under large roughness condition, the skin friction factor can also be defined as a function of δ/k_s, where δ is y distance at $U = 0.99U_e$. The relationship between C_f and δ/k_s is shown in Fig. 5a, which shows that, in all cases, C_f decreases with the increase in δ/k_s, and this trend is consistent with small roughness conditions in the literature.

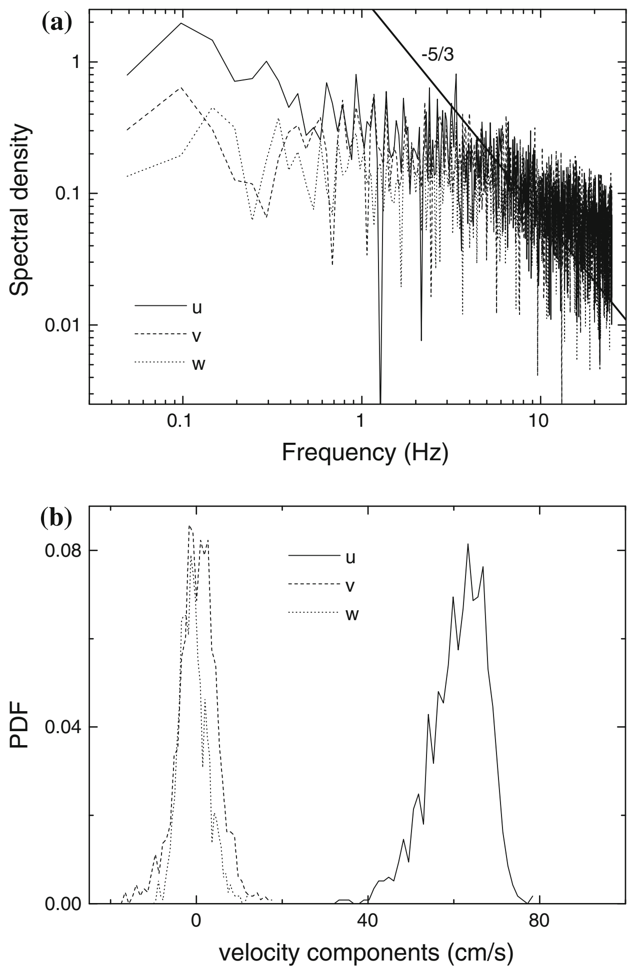

Fig. 2 **a** Relationship between the power spectrum of velocity and frequency. **b** Relationship between probability density function (PDF) and velocity components (Run 8, distance above bed is 4.99 cm)

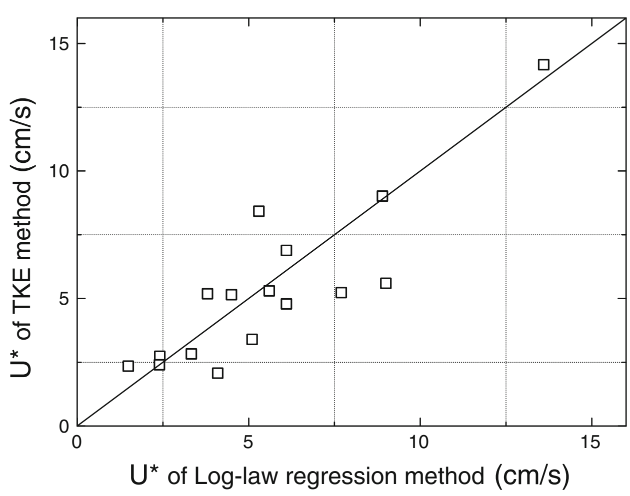

Fig. 3 Shear velocity calculated using two methods

According to boundary-layer theory, the momentum boundary-layer thickness θ is estimated from the equation $\theta = \int_0^\infty \frac{U}{U_e}\left(1 - \frac{U}{U_e}\right)\mathrm{d}y$. The relationship between C_f and

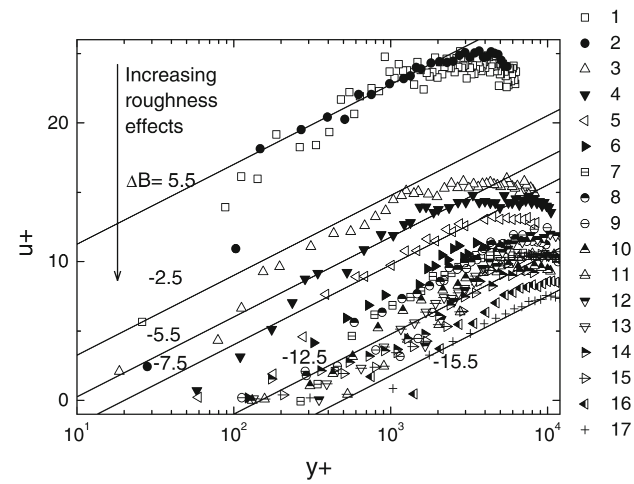

Fig. 4 Time-averaged velocity profiles

Re_θ is shown in Fig. 5b. It should be noted that gravel bed data spans a wide range of Re_θ. For smooth walls, the skin friction can be used to estimate the flow resistance, while in gravel beds, resistance will be dominated by either micro-bed forms or small-scale morphological features such as pebble clusters (Hassan and Reid 1990; Lawless and Robert 2001; Jay Lacey and Roy 2007). Therefore, this offers only an overall COR relationship between roughness effect and hydraulic conditions.

3.3 Reynolds stress

Reynolds normal stresses are shown in Fig. 6 in outer scaling as suggested in the literature (Akinlade et al. 2004; Newhall 2006; Brzek et al. 2007). The turbulence characteristics of Run1 and Run2 are identical; therefore the results of Run1 have been removed. For $k_s^+ \leq 47$, the longitudinal and lateral Reynolds stresses reach a peak near the wall and then decrease gradually. For rougher surfaces, the peak values of $\overline{u'^2}^+$ decrease gradually with the increase in k_s^+. As the roughness increases, the peak values decrease from 8.2 to 0.8. It should be noted that the normalized values depend strongly on the estimation of shear velocity. This also indicates that the $\overline{u'^2}^+$ is larger than $\overline{v'^2}^+$, and both display significant differences for different k_s^+ values. Both $\overline{u'^2}^+$ and $\overline{v'^2}^+$ fit the exponential distribution in outer region, but $\overline{w'^2}^+$ fits only at large roughness. As stated by Nezu and Nakagawa (1993), the roughness effect on turbulence can be predicted with the increase of roughness size as the tendency toward isotropy. Previous studies (Wang 1991; Wang et al. 1993; Yang et al. 2009) also reported that roughness caused flow turbulence to be well distributed. In this study, the components of Reynolds stress tend to be more isotropic with the increase in k_s^+,

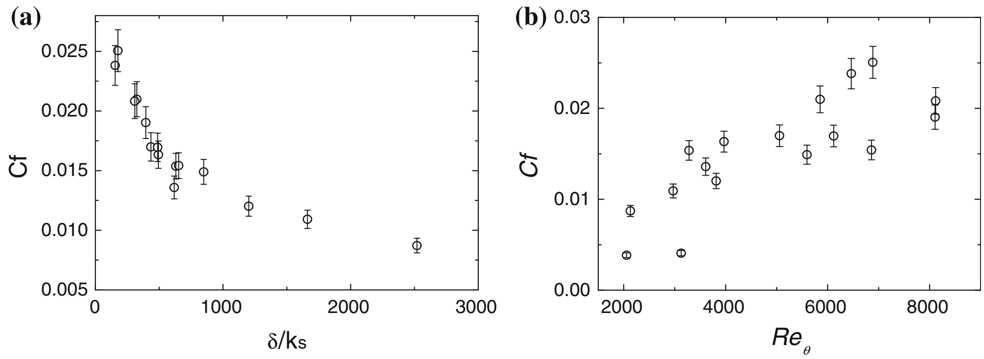

Fig. 5 Relationship between skin friction and **a** ratio of rough-wall momentum boundary-layer thickness to roughness height, **b** Reynolds number Re_θ (overall uncertainty in C_f: ±7%)

which are contrary to the observations reported by Hong et al. (2011) and demands systematic investigation to decide the debate. The distributions of Reynolds shear stress, as shown in Fig. 7, essentially reflect the COR of the fluctuating velocity components between u' and w'. This shows that the influence of roughness on turbulent stresses can be felt from the roughness layer up to the outer region. This is consistent with the work of Krogstad et al. (1992) and leads to a challenge to the wall similarity hypothesis.

The roughness effects can be explained from the redistribution of turbulent energy (Nezu and Nakagawa 1993). Quadrants analysis can also be used to determine macro-turbulent structure (Shvidchenko and Pender 2001; Brzek et al. 2007; Cal et al. 2009). Figure 8 depicts the quadrant distribution of flow velocity fluctuations between u' and w'. In Fig. 8a, the monitoring point is 2.85 cm above bed, and the flow tends to be in an equilibrium status, while in Fig. 8b, the monitoring point is 17.35 cm above bed, with low speed ejection and high speed sweep motions (Paiement-Paradis et al. 2003; Hardy et al. 2009). Identical to the results of Kim et al. (1987), the low-speed sweep motions are $u' < 0$, $w' > 0$ and high-speed ejection motions are $u' > 0$ and $w' < 0$. Both the sweep from the second quadrant and ejection from the fourth quadrant produce positive Reynolds stress, which is responsible for the turbulence redistribution in the roughness layer.

3.4 Higher-order turbulence moments

The skewness $S_{u'}$ of the fluctuating velocity component is defined as the third moment normalized by the third-order root mean square σ.

$$S_{u'} = \overline{u'^3}/\sigma^3 \tag{3}$$

This variable can be used to analyze the momentum transport process. Figure 9 presents the skewness of the three fluctuating velocity components, $S_{u'}$, $S_{v'}$, $S_{w'}$. It can be seen from Fig. 9 that $S_{u'}$ and $S_{v'}$ follow the same trend, while $S_{w'}$ changes its trend when $k_s^+ > 47$, which suggests that the roughness influences mainly $S_{w'}$. The trends of $S_{u'}$ and $S_{w'}$ are identical to the DNS results of Kim et al. (1987), while $S_{v'}$ is slightly different. This indicates that $S_{u'}$ presents different sensitivity to wall conditions compared with other two products and that $S_{w'}$ is more sensitive. This also implies that the roughness in near wall region causes the flow structure to tend to be three-dimensional, and that the vertical direction is the most easily affected. According to Raupach (1981), skewness is independent of the surface roughness except in a layer close to the wall. But Bhaganagar et al. (2004) stated that the instantaneous velocity skewness followed the same trend for both smooth and rough walls throughout the boundary layer, and that skewness was an insensitive parameter when determining changes in large-scale structures of the outer layer region. In this study, we found that rough surface affects the turbulent transport of Reynolds stress even in the outer region (see Fig. 9). In the work of Antonia and Krogstad (2001) and Bigillon et al. (2006), a change in sign of $S_{u'}$ in the near wall region also occurred, and was attributed to differences in wall roughness conditions. In addition to the skewness, studies on the triple products of normalized fluctuating velocity $\overline{u'^3}^+ = \overline{u'^3}/U_\tau^3$ have also provided valuable information. Krogstad and Antonia (1999) carried out experiments using mesh and rod roughness, and suggested that the $\overline{u'^3}^+$ should not show the same sensitivity to wall conditions as the other two triple products when y/d (d is the rod diameter) is larger than 0.1. Schultz and Flack (2007) observed that the velocity triple products $\overline{u'^3}^+$ change sign near roughness, while $\overline{v'^3}^+$ were independent of roughness.

4 Conclusions

Due to the extreme complication of turbulence mechanisms, extensive experiments should be carried out to

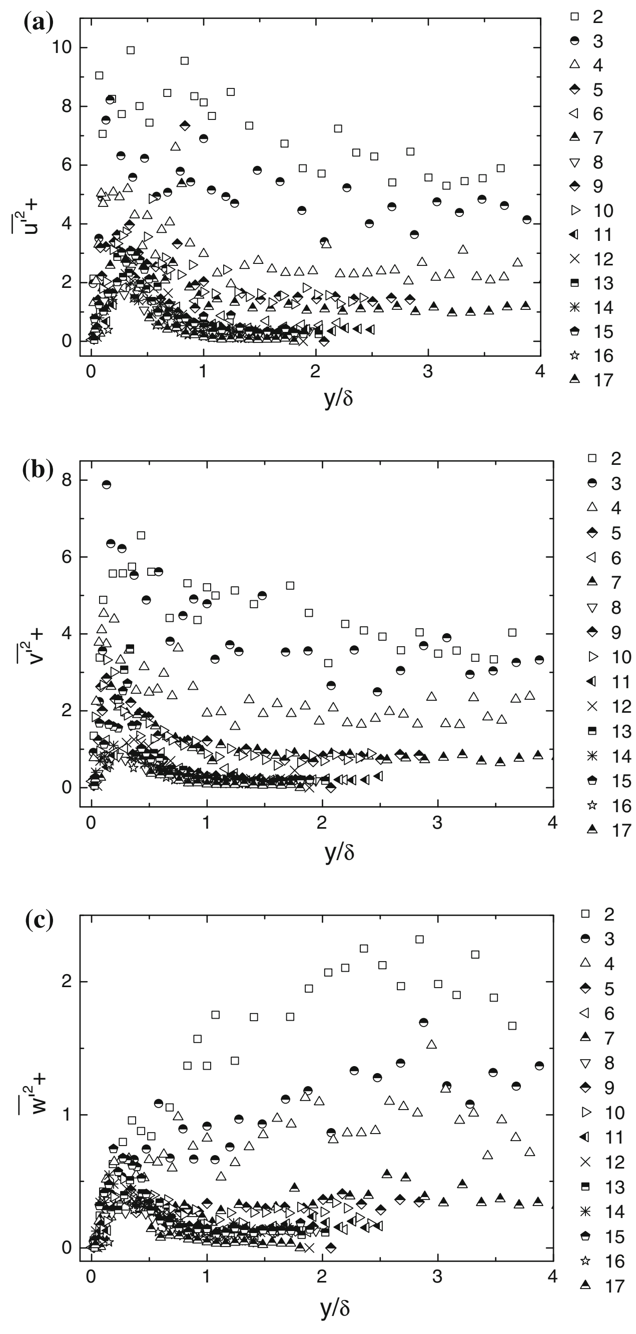

Fig. 6 Normalized Reynolds stresses distributions. **a** $\overline{u'^2}^+$; **b** $\overline{v'^2}^+$; **c** $\overline{w'^2}^+$ (Overall uncertainty: ±5%)

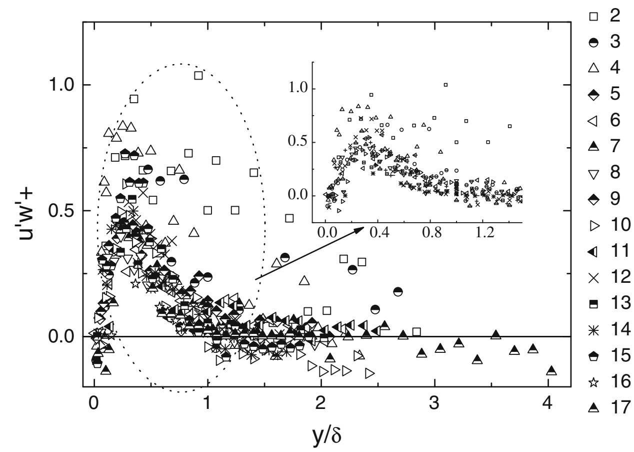

Fig. 7 Reynolds shear stress distribution (overall uncertainty: ±5%)

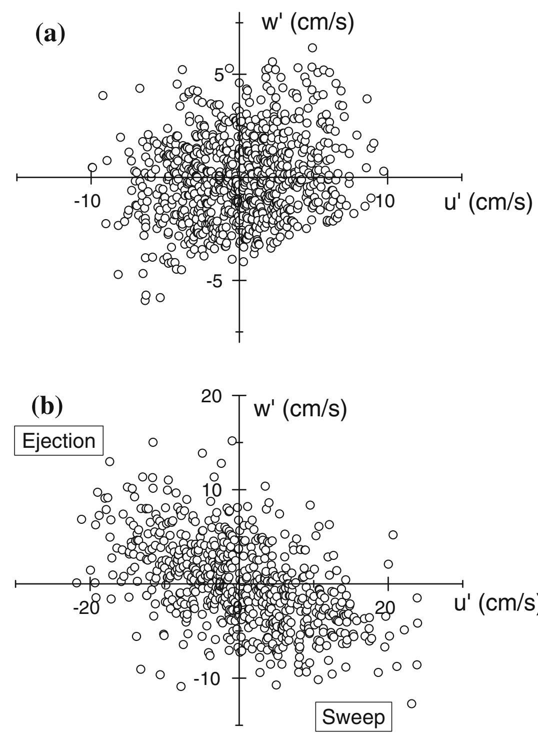

Fig. 8 Quadrant plots of longitudinal and vertical flow velocity fluctuations of Run 15. **a** $h = 2.85$ cm; **b** $h = 17.35$ cm (overall uncertainty: ±1%)

completely understand this issue. In order to properly predict flow characteristics, experimental results need to be analyzed and examined carefully. In this study, the mean flow characteristics and turbulent parameters were investigated in detail via experiments. The results yielded the velocity profiles and distributions of statistical parameters in the gravel bed.

Although the velocity profile fits well with log-law in hydraulically rough flow, the hold region and roughness function depend not only on the roughness elements but also on the flow conditions. Skin friction has a close relationship with momentum boundary-layer thickness and Reynolds number. The turbulent characteristics can be used to examine the classical wall similarity hypothesis in gravel bed roughness. The friction velocity in the gravel bed can be estimated from two methods, i.e., the logarithmic profile method and the turbulent-kinetic energy method. The Reynolds stresses in the gravel bed are less than those in smooth surfaces and show a dependence on roughness

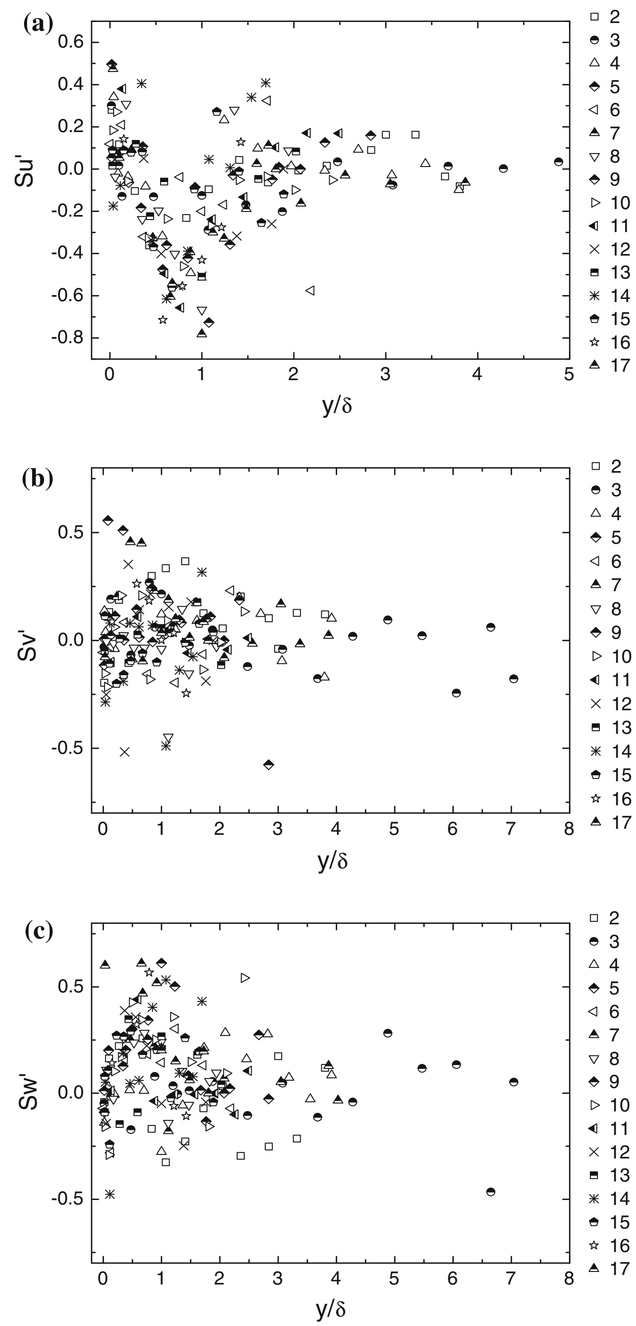

Fig. 9 Distributions of third moments in outer scaling (overall uncertainty: ±5%)

condition. In addition, the third moments of the fluctuating velocity components show an identical trend between longitudinal and lateral direction and a different trend in vertical direction. Moreover, gravel bed roughness can influence turbulent transport, especially in the vertical direction.

Combined with numerical simulations, further studies should be performed to better explore the effects of roughness, especially adjacent to a wall. Moreover, the above results, if considered in a turbulence model, can be applied to a wide range of industrial projects.

Acknowledgments The work described in this paper was supported partially by a Strategic Research Grant from the City University of Hong Kong, Hong Kong Special Administrative Region, HKSAR [Project No. 7002684(BC)], and the National Natural Science Foundation of China (Grant No. 40771022).

References

Antonia RA, Krogstad P-A (2001) Turbulence structure in boundary layers over different types of surface roughness. Fluid Dyn Res 28:139–157

Akinlade DB, Bergstrom DJ, Tachie MF, Castillo L (2004) Outer flow scaling of smooth and rough wall turbulent boundary layers. Exp Fluids 37(4):604–612

Antonia RA (2001) Turbulence structure in boundary layers over different types of surface roughness. Fluid Dyn Res 28(2):139–157

Bakken OM, Krogstad P, Ashrafian A, Andersson HI (2005) Reynolds number effects in the outer layer of the turbulent flow in a channel with rough walls. Phys Fluids 17(6):065101

Bandypadhyay PR, Watson RD (1988) Structure of rough-wall turbulent boundary layers. Phys Fluids 31(7):1877–1883

Bhaganagar K, Kim J, Coleman G (2004) Effect of roughness on wall-bounded turbulence.Flow Turbulence Combust 72:463–492

Bigillon F, Niño Y, Garcia MH (2006) Measurements of turbulence characteristics in an open-channel flow over a transitionally-rough bed using particle image velocimetry. Exp Fluids 41(6):857–867

Biron PM, Lane SN, Roy AG, Bradbrook KF, Richards KS (1998) Sensitivity of bed shear stress estimated from vertical velocity profiles: the problem of sampling resolution. Earth Surf Proc Land 23(2):133–139

Blocken B, Stathopoulos T, Carmeliet J (2007) CFD simulation of the atmospheric boundary layer: wall function problems. Atmos Environ 41(2):238–252

Brzek B, Cal RB, Johansson G, Castillo L (2007) Inner and outer scalings in rough surface zero pressure gradient turbulent boundary layers. Phys Fluids 19(6):065101

Buffin-Belanger T, Roy AG (2005) 1 min in the life of a river: selecting the optimal record length for the measurement of turbulence in fluvial boundary layers. Geomorphology 68:77–94

Cal RB, Brzek B, Johansson TG, Castillo L (2009) The rough favourable pressure gradient turbulent boundary layer. J Fluid Mech 641:129–155

Carollo FG, Ferro V, Termini D (2005) Analyzing turbulence intensity in gravel bed channels. J Hydraul Eng 131(12):1050–1061

Castillo L, Seo J, Hangan H, Johansson TG (2004) Smooth and rough turbulent boundary layers at high Reynolds number. Exp Fluids 36(5):759–774

Dean RB (1978) Reynolds number dependence of skin friction and other bulk flow variables in two-dimensional rectangular duct flow. J Fluid Eng 100:215–223

Dey S, Lambert MF (2005) Reynolds stress and bed shear in nonuniform unsteady open-channel flow. J Hydraul Eng 131(7):610–614

Ferro V (1999) Friction factor for gravel-bed channel with high boulder concentration. J Hydraul Eng 125(7):771–778

Ferro V (2003a) Flow resistance in gravel-bed channels with large-scale roughness. Earth Surf Proc Land 28(12):1325–1339

Ferro V (2003b) ADV measurements of velocity distributions in a gravel-bed flume. Earth Surf Proc Land 28(7):707–722

Ferro V, Baiamonte G (1994) Flow velocity profiles in gravel-bed rivers. J Hydraul Eng 120(1):60–80

Ferro V, Giordano G (1991) Experimental study of flow resistance in gravel-bed rivers. J Hydraul Eng 117(10):1239–1246

Flack KA, Schultz MP, Shapiro TA (2005) Experimental support for Townsend's Reynolds number similarity hypothesis on rough walls. Phys Fluids 17(3):035102

Flack K, Schultz MS, Connelly JS (2007) Examination of a critical roughness height for outer layer similarity. Phys Fluids 19(9):095104

Franca MJ (2005) A field study of turbulent flows in shallow gravel-bed rivers. PhD thesis, École Polytechnique Fédérale De Lausanne, Portugal

Hardy RJ, Best J, Lane SN, Carbonneau PE (2009) Coherent flow structures in a depth-limited flow over a gravel surface. The role of near-bed turbulence and influence of Reynolds number. J Geophys Res 113:F01003

Hassan MA, Reid I (1990) The influence of microform bed roughness elements on flow and sediment transport in gravel bed rivers. Earth Surf Proc Land 15(8):739–750

Hong J, Katz J, Schultz MP (2011) Near-wall turbulence statistics and flow structures over three-dimensional roughness in a turbulent channel flow. J Fluid Mech 667:1–37

Jay Lacey RW, Roy AG (2007) A comparative study of the turbulent flow field with and without a pebble cluster in a gravel bed river. Water Resour Res 43:W05502

Jimenez J (2004) Turbulent flows over rough walls. Annu Rev Fluid Mech 36(1):173–196

Kim J, Moin P, Moser RD (1987) Turbulence statistics in fully developed channel flow at low Reynolds number. J Fluid Mech 177:133–166

Kim S-C, Friedrichs CT, Maa JP-Y, Wright LD (2000) Estimating bottom stress in tidal boundary layer from acoustic Doppler velocimeter data. J Hydraul Eng 126(6):399–406

Kirkbride A (1993) Observations of the influence of bed roughness on turbulence structure in depth limited flows over gravel beds. In: Clifford NJ, French JR, Hardisty J (eds) Turbulence: perspectives on flow and sediment transport. Wiley, Chichester, pp 185–196

Kirkbride AD, McLelland SJ (1994) Visualization of the turbulent-flow structure in a gravel-bed river. Earth Surf Proc Land 19(9):819–825

Krogstad P-A, Antonia RA, Browne WB (1992) Comparison between rough- and smooth-wall turbulent boundary layers. J Fluid Mech 245:599–617

Krogstad P-A, Antonia RA (1999) Surface roughness effects in turbulent boundary layers. Exp Fluids 27(55):450–460

Lane SN, Biron PM, Bradbrook KF, Butler JB, Chandler JH, Crowell MD et al (1998) Three-dimensional measurement of river channel flow processes using acoustic Doppler velocimetry. Earth Surf Proc Land 23(13):1247–1267

Lawless M, Robert A (2001) Three-dimensional flow structure around small-scale bedforms in a simulated gravel-bed environment. Earth Surf Proc Land 26(5):507–522

Leonardi S, Orlandi P, Antonia RA (2005) A method for determining the frictional velocity in a turbulent channel flow with roughness on the bottom wall. Exp Fluids 38(6):796–800

Lopez F, Garcia MH (1999) Wall similarity in turbulent open-channel flow. J Eng Mech 125(7):789–796

Lu WZ, Leung AYT (2003) A preliminary study on potential of developing shower/laundry wastewater reclamation and reuse system. Chemosphere 52:1451–1459. doi:10.1016/S0045-6535(03)00482-X

Lyn DA (1993) Turbulence measurements in open-channel flows over artificial bed forms. J Hydraul Eng 119(3):306–326

McLelland SJ, Nicholas AP (2000) A new method for evaluating errors in high-frequency ADV measurements. Hydrol Process 14(2):351–366

Nagib HM, Christophorou C, Monkewitz PA (2006) High Reynolds number turbulent boundary layers subjected to various pressure-gradient condition. In: Meier GEA, Sreenivasan KR (eds) IUTAM symposium on 100 years of boundary layer research, pp 383–394

Nakagawa H, Nezu I, Ueda H (1975) Turbulence of open channel flow over smooth and rough beds. Proc Jpn Soc Civil Eng 241:155–168

Newhall KA (2006) Turbulent boundary layers: a look at skin friction, pressure gradient, surface roughness and the power law. Masters thesis, Rensselaer Polytechnic Institute, New York

Nezu I, Nakagawa H (1993) Turbulence in open-channel flows IAHR monograph. Balkema, Rotterdam

Nezu I, Rodi W (1986) Open-channel flow measurements with a laser Doppler anemometer. J Hydraul Eng ASCE 112(5):411–429

Nikora VI, Smart GM (1997) Turbulence characteristics of New Zealand gravel-bed rivers. J Hydraul Eng 123(9):764–773

Nikora VI, Goring DG, Biggs BJ (1998) ADV measurements of turbulence: can we improve their interpretation. J Hydraul Eng 124(6):630–634

Paiement-Paradis G, Buffin-Belanger T, Roy AG (2003) Scalings for large turbulent flow structures in gravel-bed rivers. Geophys Res Lett 30(14):1773, doi:10.1029/2003GL017553

Perry AE, Schofield WH, Joubert PN (1969) Rough wall turbulent boundary layers. J Fluid Mech 37(2):383–413

Raupach MR (1981) Conditional statistics of Reynolds stress in rough-wall and smooth-wall turbulent boundary layers. J Fluid Mech 108:363–382

Schlichting H (1979) Boundary-layer theory, 7th edn. McGraw-Hill, New York

Schultz MP, Flack KA (2005) Outer layer similarity in fully rough turbulent boundary layers. Exp Fluids 38:328–340

Schultz MP, Flack KA (2007) The rough-wall turbulent boundary layer from the hydraulically smooth to the fully rough regime. J Fluid Mech 580:381–405

Sheng J, Malkiel E, Katz J (2008) Using digital holographic microscopy for simultaneous measurements of 3D near wall velocity and wall shear stress in a turbulent boundary layer. Exp Fluids 45(6):1023–1035

Shocking MA, Allen JJ, Smits AJ (2006) Roughness effects in turbulent pipe flow. J Fluid Mech 564:267–285

Shvidchenko AB, Pender G (2001) Macroturbulent structure of open-channel flow over gravel beds. Water Resour Res 37(3):709–719

Smart GM (1999) Turbulent velocity profiles and boundary shear in gravel bed rivers. J Hydraul Eng 125(2):106–116

Song T, Chiew YM, Mechanics E (2001) Turbulence measurement in nonuniform open-channel flow using acoustic Doppler velocimeter (ADV). J Eng Mech 127(3):219–232

Stone M, Tritico H, Hotchkiss R, Flanagan P (2003) Turbulence characteristics in obstructed gravel bed flow. In 16th ASCE engineering mechanics conference, Seattle, pp 1–6

Tachie M, Bergstrom D, Balachandar R (2000) Rough wall turbulent boundary layers in shallow open channel flow. J Fluid Mech 122:533–541

Townsend AA (1976) The structure of turbulent shear flow. Cambridge University Press, Cambridge

Tritico HM, Hotchkiss RH (2005) Unobstructed and obstructed turbulent flow in gravel bed rivers. J Hydraul Eng 131(8):635–645

van Rijn LC (1982) Equivalent roughness of alluvial bed. J Hydraul Div Am Soc Civ Eng 108(10):1215–1218

Volino RJ, Schultz MP, Flack KA (2007) Turbulence structure in rough- and smooth-wall boundary layers. J Fluid Mech 592:263–293

Volino RJ, Schultz MP, Flack KA (2009) Turbulence structure in a boundary layer with two-dimensional roughness. J Fluid Mech 635:75–101

Voulgaris G, Trowbridge JH (1998) Evaluation of the acoustic Doppler velocimeter (ADV) for turbulence measurements. J Atmos Ocean Tech 15(1):272–289

Wang J–J (1991) Distribution of turbulent intensity in a gravel-bed flume. Exp Fluids 11(2–3):201–202

Wang JJ, Dong Z (1996) Open-channel turbulent flow over non-uniform gravel beds. Appl Sci Res 56(4):243–254

Wang JJ, Dong ZN, Chen CZ, Xia ZH (1993) The effects of bed roughness on the distribution of turbulent intensities in open-channel flow. J Hydraul Res 31(1):89–98

Wosnik M, Castillo L, George WK (2000) A theory for turbulent pipe and channel flows. J Fluid Mech 42(1):115–145

Wu Y, Christensen KT (2007) Outer-layer similarity in the presence of practical rough-wall topography. Phys Fluids 19(8):085108

Yang QY, Wang XY, Lu WZ, Wang XK (2009) Experimental study on characteristics of separation zone in confluence zone in rivers. J Hydrol Eng 14(2):166–177. doi:10.1061/(ASCE)1084-0699(2009)14:2(166)

Zanoun E, Durst F, Nagib H (2003) Evaluating the law of the wall in two-dimensional fully developed turbulent channel flows. Phys Fluids 15(10):3079–3089